ARMY RESEARCH LABORATORY

Observation of an Ultrahard Phase of Graphite Quenched from High-pressure

by Jennifer A. Ciezak-Jenkins

ARL-TR-5466 **February 2011**

Approved for public release; distribution unlimited.

NOTICES

Disclaimers

The findings in this report are not to be construed as an official Department of the Army position unless so designated by other authorized documents.

Citation of manufacturer's or trade names does not constitute an official endorsement or approval of the use thereof.

Destroy this report when it is no longer needed. Do not return it to the originator.

Army Research Laboratory
Aberdeen Proving Ground, MD 21005-5069

ARL-TR-5466 **February 2011**

Observation of an Ultrahard Phase of Graphite Quenched from High-pressure

Jennifer A. Ciezak-Jenkins
Weapons and Materials Research Directorate, ARL

Approved for public release; distribution unlimited.

REPORT DOCUMENTATION PAGE	Form Approved OMB No. 0704-0188

Public reporting burden for this collection of information is estimated to average 1 hour per response, including the time for reviewing instructions, searching existing data sources, gathering and maintaining the data needed, and completing and reviewing the collection information. Send comments regarding this burden estimate or any other aspect of this collection of information, including suggestions for reducing the burden, to Department of Defense, Washington Headquarters Services, Directorate for Information Operations and Reports (0704-0188), 1215 Jefferson Davis Highway, Suite 1204, Arlington, VA 22202-4302. Respondents should be aware that notwithstanding any other provision of law, no person shall be subject to any penalty for failing to comply with a collection of information if it does not display a currently valid OMB control number.
PLEASE DO NOT RETURN YOUR FORM TO THE ABOVE ADDRESS.

1. REPORT DATE *(DD-MM-YYYY)*	2. REPORT TYPE	3. DATES COVERED (From - To)
February 2011	Final	1 October 2009 to 30 August 2010

4. TITLE AND SUBTITLE
Observation of an Ultrahard Phase of Graphite Quenched from High-pressure

5a. CONTRACT NUMBER

5b. GRANT NUMBER

5c. PROGRAM ELEMENT NUMBER

6. AUTHOR(S)
Jennifer A. Ciezak-Jenkins

5d. PROJECT NUMBER

5e. TASK NUMBER

5f. WORK UNIT NUMBER

7. PERFORMING ORGANIZATION NAME(S) AND ADDRESS(ES)
U.S. Army Research Laboratory
ATTN: RDRL-WML-B
Aberdeen Proving Ground, MD 21005-5069

8. PERFORMING ORGANIZATION REPORT NUMBER
ARL-TR-5466

9. SPONSORING/MONITORING AGENCY NAME(S) AND ADDRESS(ES)

10. SPONSOR/MONITOR'S ACRONYM(S)

11. SPONSOR/MONITOR'S REPORT NUMBER(S)

12. DISTRIBUTION/AVAILABILITY STATEMENT
Approved for public release; distribution unlimited.

13. SUPPLEMENTARY NOTES

14. ABSTRACT
In-situ isothermal high-pressure synchrotron x-ray diffraction, and optical Raman spectroscopy were used to examine the structural properties, equation of state, and vibrational dynamics of highly ordered pyrolytic graphite. The x-ray measurements show that the pressure-volume relations remain smooth to near 5.9 GPa, where there is an abrupt discontinuity. This discontinuity is correlated to a hexagonal-to-monoclinic phase transition, which was previously predicted via ab initio crystal structure algorithms. However, discontinuities in the Raman vibrational modes do not appear until near 19 GPa. The discrepancy in the onset pressure of the phase transition is correlated to edge effects. The high-pressure monoclinic phase was recovered to ambient pressure and remains stable for long periods.

15. SUBJECT TERMS
High-pressure, diamond anvil cell, pyrolytic graphite, ultrahard materials

16. SECURITY CLASSIFICATION OF:			17. LIMITATION OF ABSTRACT	18. NUMBER OF PAGES	19a. NAME OF RESPONSIBLE PERSON
a. REPORT	b. ABSTRACT	c. THIS PAGE			Jennifer A. Ciezak-Jenkins
Unclassified	Unclassified	Unclassified	UU	22	19b. TELEPHONE NUMBER (*Include area code*) (410) 278-6169

Standard Form 298 (Rev. 8/98)
Prescribed by ANSI Std. Z39.18

Contents

List of Figures

List of Tables

Acknowledgments

The Geophysical Laboratory of the Carnegie Institution of Washington is thanked for access to their high-pressure gas loading facility. The Advanced Light Source is supported by the Director, Office of Science, Office of Basic Energy Sciences of the U.S. Department of Energy under contract no. DE-AC02-05CH11231.

INTENTIONALLY LEFT BLANK.

1. Introduction

The search for ultrahard materials, which may have mechanical properties that rival or exceed that of diamond, has stimulated research under extreme conditions for over 50 years (*1*). Recent studies of simple materials under thermomechanical extremes of pressure and temperature have revealed extraordinary physical and chemical behavior accompanied by unexpectedly complex structures that were not envisioned by conventional chemical models (see, for example, references 2–7). The general theories that describe these transformations and permit extrapolation to rationally design novel materials with exotic properties are unknown. It is only through the development of new fundamental physics-based principles that the capability to manipulate the structures of elements and compounds into novel, yet practical, materials will be achieved. Innovative experiments coupled with state-of-the-art computational simulations are needed to not only describe this unique behavior, but to provide a framework for making useful and accurate predictions. By studying the formation of exotic phases of materials under extreme conditions, an understanding of how to predict and ultimately influence metastability will be developed; such capability is an important first step in understanding how material properties can be manipulated and exploited to design new, novel, and improved materials that cannot be obtained through conventional synthesis approaches. Such materials, particularly those made of first and second row elements, represent an entirely new class of materials that may exhibit many interesting properties of relevance to Department of Defense (DoD) interests, such as super-hardness (*4 ,8*), optical nonlinearity (*2*) and high-energy-density (*2, 3, 5*).

This work examines the synthesis, physical and chemical properties, metastability, and recovery mechanism of an ultrahard phase of carbon, formed from isothermal compression of pyrolytic graphite. Materials with bulk moduli and a hardness rivaling that of diamond have been theoretically predicted for many years (see, for example, references 9–11) but the existence of ultrahard phases of carbon has only recently been experimentally documented under extreme conditions in graphite (*4, 7*), nanotubes (*12*), and fullerenes (*13*). It is well known that polycrystalline graphite, shown in figure 1, undergoes a structural phase transition slightly above 16 GPa at room temperature; this transition is accompanied by striking changes in several physical and chemical properties, including electrical and optical reflectivity (*14*), x-ray diffraction (XRD) patterns, and hardness (*4, 7*). It has been speculated that the hardness of the high-pressure phase of polycrystalline graphite is comparable to or slightly exceeds that of bulk diamond, due to the indentations left by the transformed material on the planar surface of the diamond anvil upon decompression (*4*). Attempts to quench the ultrahard high-pressure phase of graphite to ambient conditions were unsuccessful (*4*). Although several potential crystallographic structures were proposed, such as hexagonal or amorphous diamond (*15–18*), experiments gave largely conflicting results as to the actual crystallographic structure. Recent ab initio crystal structure predictions (*7*) have shown a close correlation between the simulated

properties of a monoclinic carbon phase, shown in figure 2, and those derived from experimental measurements (*4*), including the optical transparency and sharp drop in reflectivity after the phase transition. The simulations have also suggested the hardness (83.1 GPa) and bulk modulus (431.2 GPa) of the monoclinic material are comparable to diamond; however, this report gave no insights into possible mechanisms to introduce metastability into the material (*7*). In this work, the synthesis of a quenchable high-pressure monoclinic carbon phase formed by cold compression of highly ordered pyrolytic graphite (HOPG) is detailed. XRD and Raman spectroscopic data clearly confirm a significant change in the physical properties of the pyrolytic graphite material after the phase transition, which remain after a quench to ambient conditions.

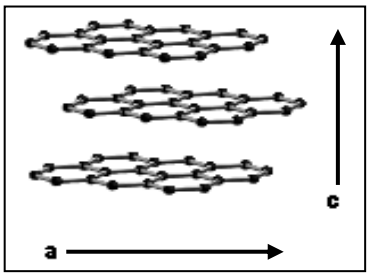

Figure 1. Graphite model, showing the planar orientation.

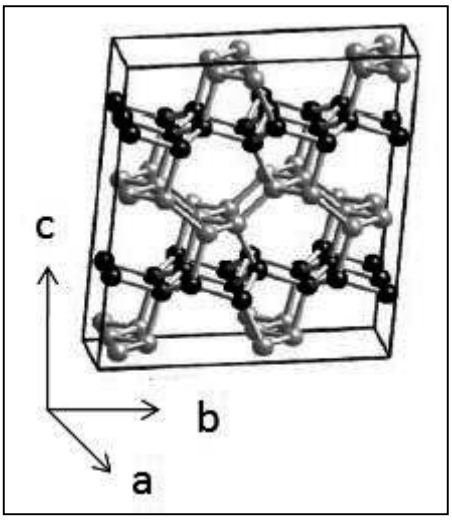

Figure 2. Ab initio predicted crystal structure of monoclinic carbon. Reproduced directly from reference 7.

2. Experimental Methodology

Grade ZYA HOPG was purchased from SPI Supplies and used without further purification. A flake of approximately 50 microns in diameter and a thickness of 20 microns was removed from

the larger SPI sample and positioned in a piston-cylinder-type diamond anvil cell equipped with 300-micron diamond culets and a stainless steel gasket. For both the Raman spectroscopic and XRD measurements a neon pressure medium was loaded into the diamond anvil cell using a specialized high-pressure gas loading system (*19*). The in-situ pressure within the diamond anvil cell was determined from the frequency shift of the ruby R_1 luminescence of several micrometer sized rubies placed around the sample (*20*). In-situ Raman scattering measurements were conducted using a diode-pumped solid-state laser operating at 532 nm and a laser spot diameter of ~4 μm. Prior to the experimental measurements, the spectrograph was calibrated using a neon lamp. This method of calibration has an accuracy of ±1 cm^{-1}. The spectral resolution for all Raman measurements was ±4 cm^{-1}.

Room temperature isothermal angle dispersive x-ray powder microdiffraction experiments were conducted on beamline 12.2.2 of the Advanced Light Source by using focused monochromatic x-rays (λ = 0.4959 Å) and a high-resolution image plate detector. The recorded two-dimensional diffraction images were then integrated to produce high-quality angle dispersive XRD patterns using FIT2D.

3. Results

3.1 X-ray Diffraction

HOPG is a unique polycrystalline polymorph of graphite with a hexagonal structure of planar layers and a high degree of preferred orientation. The lattice parameters for the hexagonal cell of HOPG at ambient conditions are $a = c = 3.42$ Å. Good agreement of the XRD patterns with previously reported results (*21*) was noted, with five characteristic diffraction peaks below 20° at 0.5 GPa: (111), (201), (112), (202), and (203). To understand the high-pressure behavior of HOPG, XRD upon isothermal compression was measured at room temperature and several representative XRD patterns are shown in figure 3. Upon compression to 5.9 GPa, a discontinuous change in the XRD patterns was observed, but the Bragg peaks observed at 0.5 GPa remained traceable to the original pattern, indicating that the high-pressure form remained in a graphite-like atomic rearrangement and was not amorphous. The appearance of several new peaks at 5.9 GPa suggests at least a partial phase transition to a crystallographic symmetry lower than hexagonal. These new peaks were indexed on the basis of the monoclinic symmetry proposed by Li et al. (*7*) as (201), (202), (–203), (220), (420), and (620). In contrast to Mao et al. (*4*), the onset of this transition began near 5.9 GPa. However, between 5.9 and 12.2 GPa, the *a* and *c* lattice parameters do not change significantly, suggesting the phase transition from hexagonal to monoclinic is very sluggish at room temperature and, that between 5.9 and 12.2 GPa, the material can be approximately considered as a distorted hexagonal structure, as previously proposed (*4*). The lattice parameters calculated from the diffraction patterns are listed in table 1.

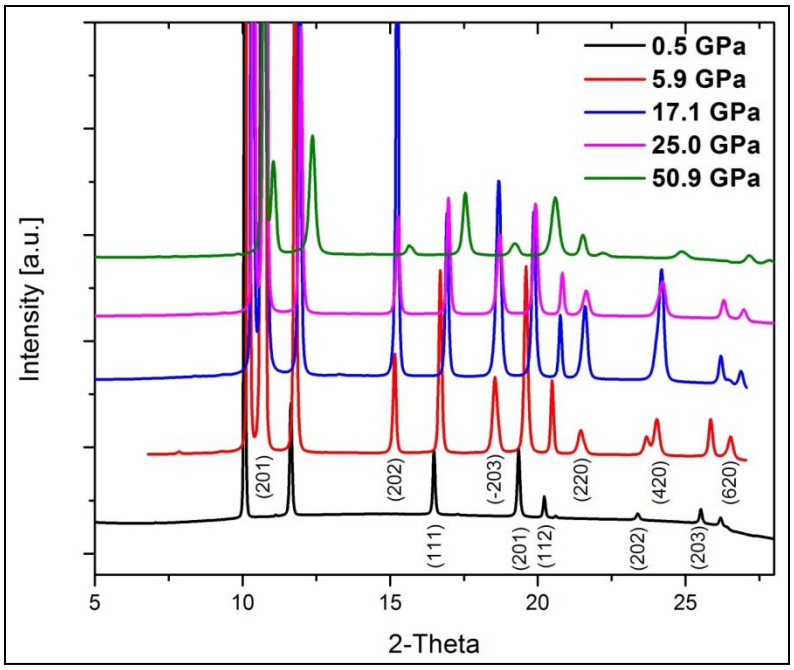

Figure 3. XRD of HOPG; the patterns are offset for clarity.

Table 1. Lattice parameters of HOPG as a function of pressure.

Pressure (GPa)	***a***	***b***	***c***	***beta***
0.0	3.42(4)		3.42(4)	
0.2	3.32(6)		3.34(5)	
2.1	3.32(1)		3.33(5)	
3.4	3.31(5)		3.31(4)	
5.9	3.09(8)		3.76(2)	102.7(2)
7.3	3.06(4)		3.74(1)	101.0(2)
12.2	3.04(1)	2.17(4)	3.71(9)	99.1(5)
15.9	3.00(0)	2.15(1)	3.67(2)	98.4(7)
18.1	2.97(3)	2.14(5)	3.62(6)	97.2(5)
22.9	2.92(5)	2.13(3)	3.60(3)	96.0(2)
29.6	2.87(7)	2.11(1)	3.57(5)	95.6(6)
33.2	2.87(1)	2.09(9)	3.55(5)	94.9(5)
42.1	2.83(4)	2.08(4)	3.48(4)	94.1(5)
50.9	2.79(3)	2.08(3)	3.43(3)	93.5(9)

The relationship between pressure and volume (P-V) of HOPG to near 51 GPa is represented in figure 4. The P-V isotherm was fit to the third-order Birch-Murnaghan equation of state (*22*):

$$P(GPa) = {}^{3}/_{2}\, B_o\, [n^{-7/3} - n^{-5/3}\,] - [1 - 3\,(1 - {}^{B'}/_{4})\,(n^{-2/3} - 1)], \qquad (1)$$

where $\eta = {}^{V}/_{Vo}$ and B_0 and B′ are the bulk modulus and its pressure derivative, respectively. The best data fits were obtained when B_0 = 432 GPa, which exceeds that of cubic boron nitride (401 GPa) and rivals that of diamond (468 GPa). Above 5.9 GPa, the smoothly varying curve shows no evidence of discontinuities that could indicate additional phase transitions.

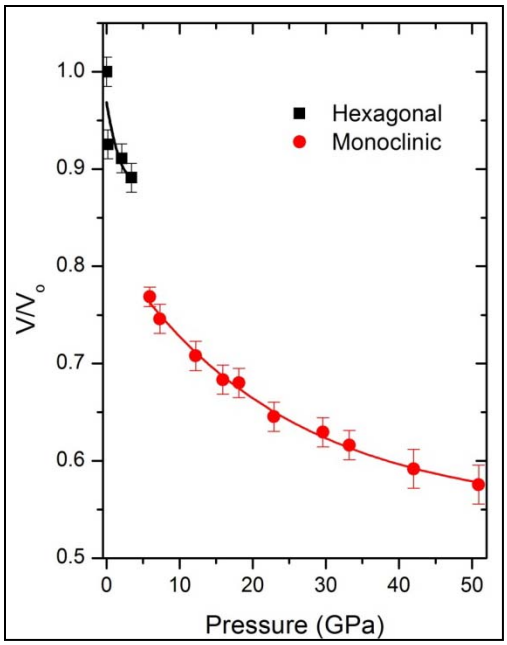

Figure 4. The P-V equation of state of cold compressed HOPG. The obvious discontinuity near 6 GPa is indicative of a phase transition. Both data sets were fit using a third-order Birch-Murnaghan equation of state (*22*).

The *a* and *c* lattice parameters of the monoclinic cell determined from the diffraction patterns give the pressure dependence of the axial ratio c/a for the unit cell, also called the anisotropic ratio. The anisotropic ratio is shown in figure 5 as a function of pressure. Above the phase transition at 5.9 GPa, the *a* and *c* values decrease smoothly with pressure, as is shown in table 1, with the *c* axis being slightly more compressible. Beginning near the phase transition at 5.9 GPa, the anisotropic ratio increases and reaches its maximum by 30 GPa. The broad pressure range associated with the increase in the anisotropic ratio suggests a sluggish phase transition, which does not near completion until near 30 GPa. The increase in the anisotropic ratio over this pressure range may be attributed to a decrease in the spacing between the planes (figure 1); at relatively low pressures, the van der Waals forces between these layers are relatively weak, permitting larger compression, whereas after the phase transition, interplanar bonds are formed between the graphene sheets. Only when the sheets buckle does the anisotropic ratio decrease. This trend has also been observed in other layered materials including tungsten disulfide (*23*), molybdenum disulfide (*24*), and uranium (*25*).

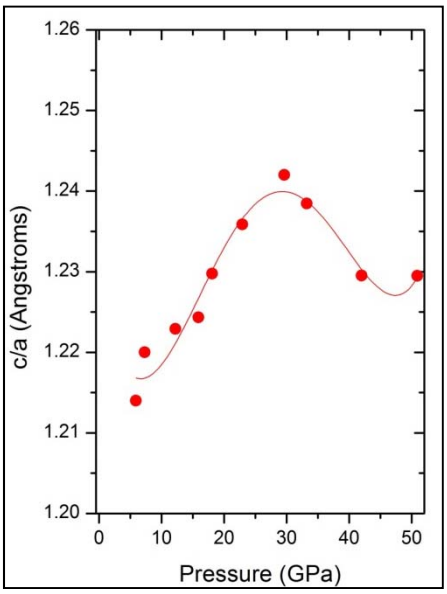

Figure 5. Anisotropic ratio of HOPG as a function of pressure.

3.2 Raman Spectroscopy

The evolution of the Raman frequencies of HOPG on isothermal compression at room temperature to near 25 GPa are shown in figure 6. The physical origin of the Raman bands in graphite is a subject of great debate; however, several general discussions regarding the symmetry selection rules in graphite are available (*26*, *27*). The main spectral features of the Raman spectra of HOPG are the so-called G and D peaks, which lie around 1590 cm^{-1} and 1795 cm^{-1}, respectively, for visible excitation. Except for when using ultraviolet (UV) excitation, Raman spectra of all graphitic carbons are dominated by the sp^2 sites, because visible excitation always resonates with the strong π bonding states of the graphene sheets (figure 1).

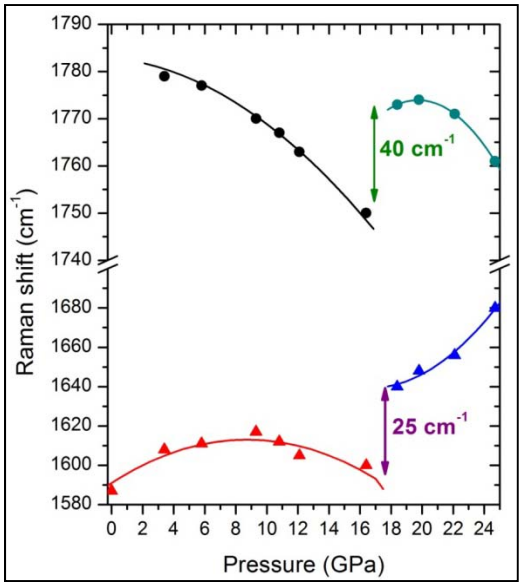

Figure 6. Raman frequency shifts of HOPG as a function of pressure. Fits were obtained using least squared analysis.

The assignment of the D and G peaks is straightforward in the molecular picture of HOPG, as these bands are present in all poly-aromatic hydrocarbons (*28, 29*). The G peak is due to the bond stretching of all pairs of sp^2 atoms in the graphite rings. The D peak is due to the breathing modes of sp^2 atoms in rings (*28, 30, 31*). While second-order scattering is, in general, allowed in HOPG, the intensities of the spectral features are weak compared with the vibrational intensities of the first-order Raman modes; therefore, the second-order features are not discussed.

The following trends in figure 6 are immediately noticeable:

1. The Raman G mode centered near 1590 cm^{-1} shifts towards slightly higher frequencies until around 10 GPa and then softens between 10 and 18 GPa. The vibrational softening of this band suggests a general weakening of the ring structures of the graphene layers, perhaps due to buckling of the layers.

2. The Raman D mode softens over the pressure range from ambient to 18 GPa, implying weakening of the graphene ring structures.

3. Slightly above 18 GPa, there is an abrupt discontinuity in the vibrational frequencies of both modes, which corresponds to a phase transition.

4. Above 19 GPa, the G mode increases in frequency, suggesting a general strengthening of a new ring structure, whereas the D mode, in general, softens suggesting a collapse of the well-defined layers and a structure that is closer packed than the original material.

Upon decompression from the Raman experiments catastrophic diamond failure occurred (figure 7). It is unclear whether the diamond failed due to issues relating to the sample or an inherent condition of the diamond anvil. Despite failure of the diamond anvil, an approximate 15 x 15 micron chip of the ultrahard monoclinic phase was able to be recovered (figure 8) to ambient conditions. Raman characterization of the semi-transparent recovered sample indicates similarities with the high pressure phase. To date, the recovered sample has remained stable under ambient conditions for several months.

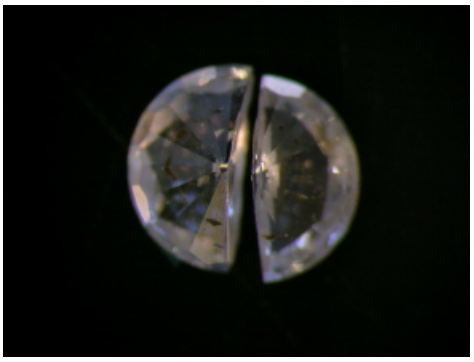

Figure 7. Cracked diamond anvil after monoclinic phase was decompressed from high-pressures.

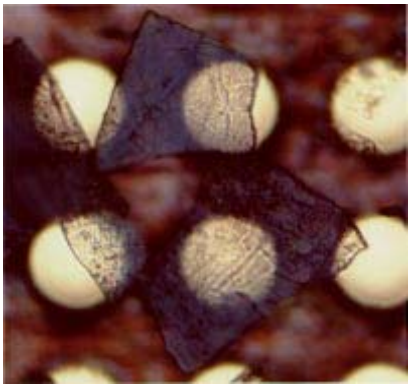

Figure 8. Approximately 15 x 15 micron HOPG sample, quenched from high-pressure, on a copper slide.

4. Discussion and Conclusions

Revolutionary ab initio crystal structure predictions by Li et al. (*7*) suggest that the well-known high-pressure phase transition in graphite is an ultrahard monoclinic polymorph of carbon. Several simulated properties, including the XRD and near K-edge inelastic x-ray scattering were compared to the experimental data of Mao et al. (*4*) and favorable agreement was noted, with the onset of the phase transition near 14 GPa. The XRD collected on HOPG in this work suggests the phase transition may near 5 GPa, due to the presence of small crystallites near the sample

edge. However, as pressure increases, additional HOPG is transformed into the new phase and can be imaged using Raman spectroscopy. In future Raman experiments, the sample will be rastered to test this hypothesis of edge effects. A similar type phenomenon is thought to occur in boron carbide, where amorphous regions grow in response to defects and pressure (*32*).

Using the monoclinic crystal structure proposed by Li et al. (*7*), the XRD peaks of HOPG were indexed to the calculated monoclinic d-spacings with an average root mean square deviation of 0.013 Å over the pressure range between 5.9 and 50.9 GPa. However, a significantly smaller *a* lattice parameter of the monoclinic phase was observed during these experiments relative to the calculated structure (*7*). This discrepancy between the computational and experimental results may be attributed to a higher degree of buckling in the graphene planes than is theoretically predicted, but additional experimental data are needed before this can be definitively concluded.

The high-pressure Raman spectroscopic results suggest that the transition is accompanied by significant destabilization of the ring structure of the graphene sheets. The G band of HOPG involves the in-plane displacements of the planar graphene sheets, while the D band involves the ring-breathing motions. We speculate that as a result of compression and the strong anisotropic properties of HOPG, the interplanar spacing decreases and there is a gradual buckling of the graphene sheets. But even more interesting is that the continued softening of the phonons above the transition suggests that the transition is not isosymmetric; it has the appearance of a zone-boundary soft mode that derives intensity from other disorder or strain. This would imply the formation of a superlattice, but additional experiments needed to be conducted before any definitive conclusions can be drawn.

The present study has provided new information on the high-pressure behavior of HOPG. Under pressure, evidence of structural changes was documented starting near 5 GPa and continuing to 19 GPa by XRD and Raman spectroscopy. On compression, both the D and G Raman modes show softening and a significant discontinuity near 19 GPa, which implies a structural transformation. Concordant with the Raman results, several new peaks appear in the XRD pattern near 5.9 GPa, which may be attributed to a phase transition. The discrepancy between the Raman and XRD has been justified as a beamsize problem; the x-ray beam, being larger, is likely sampling the edge of the sample where defects and possible seed crystals form. The pressure dependence of the c/a ratio is anomalous between 18 and 30 GPa, suggesting the phase transition is not complete until 30 GPa. The phase can be quenched to ambient conditions for extended periods of time.

5. References

1. Brazhkin, V. V.; Lyapin, A. G.; Hemley, R. J. Harder Than Diamond: Dreams and Reality. *Phil. Mag. A* **2002**, *82*, 231–253.

2. Lipp, M. J.; Evans, W. J.; Baer, B. J.; Yoo, C. S. High-energy-density Extended CO Solid. *Nature Materials* **2005**, *4*, 211–216.

3. Lipp, M. J.; Klepeis, J. P.; Baer, B. J.; Cynn, H.; Evans, W. J.; Iota, V.; Yoo, C. S. Transformation of Molecular Nitrogen to Nonmolecular Phases at Megabar Pressures by Direct Laser Heating. *Phys. Rev. B* **2007**, *76*, 014113–014118.

4. Mao, W. L.; Mao, H.-K.; Eng, P. J.; Trainor, T. P.; Newville, M.; Kao, C.-C.; Heinz, D. L.; Shu, J.; Meng, Y.; Hemley, R. J. Bonding Changes in Compressed Superhard Graphite. *Science* **2003**, *302*, 425–427.

5. Iota, V.; Yoo, C.-S.; Klepeis, J.-H.; Jenei, Z.; Evans, W. J.; Cynn, H. Six-fold Coordinated Carbon Dioxide VI. *Nature Materials* **2007**, *6*, 34–38.

6. McMillan, P. F. New Materials from High-pressure Experiments. *Nature Materials* **2002**, *1*, 19–25.

7. Li, Q.; Ma, Y.; Oganov, A. R.; Wang, H.; Wang, H.; Xu, Y.; Cui, T.; Mao, H.-K.; Zou, G. Superhard Monoclinic Polymorph of Carbon. *Phys. Rev. Lett.* **2009**, *102*, 175506–175510.

8. Oganov, A. R.; Chen, J.; Gatti, C.; Ma, Y.; Ma, Y.; Glass, C. W.; Liu, Z.; Yu, T.; Kurakevych, O. O.; Solozhenko, V. L. Ionic High-pressure Form of Elemental Boron. *Nature* **2009**, *457*, 863–868.

9. Itoh, M.; Kotani, M.; Naito, H.; Sunada, T.; Kawazoe, Y.; Adschiri, T. New Metallic Carbon Crystal. *Phys. Rev. Lett.* **2009**, *102*, 055703–055707.

10. Rignanese, G.-M.; Charlier, J.-C. Hypothetical Three-dimensional All-sp^2 Carbon Phase. *Phys. Rev. B* **2008**, *78*, 125415–125420.

11. Liu, A. Y.; Cohen, M. L.; Hass, K. C.; Tamor, M. A. Structural Properties of a Three-dimensional All-sp^2 Phase of Carbon. *Phys. Rev. B* **1991**, *43*, 6742–6745.

12. Wang, Z.; Zhao, Y.; Tait, K.; Liao, X.; Schiferl, D.; Zha, C. S.; Downs, R. T.; Qlan, J.; Zhu, Y.; Shen, T. A Quenchable Superhard Carbon Phase Synthesized by Cold Compression of Carbon Nanotubes. *Proc. Nat. Acad. Science* **2004**, *101*, 13699–13702.

13. Blank, V. D.; Buga, S. G.; Serebryanaya, N. R.; Denisov, V. N.; Dubitsky, G. A.; Ivley, A. N.; Mavrin, B. N.; Popov, M. Yu. Ultrahard and Superhard Carbon Phases Produced from C60 by Heating at High Pressure: Structural and Raman Studies. *Phys. Lett. A.* **1995**, *205*, 208–216.

14. Li, X.; Mao, H.-K. Solid Carbon at High Pressure: Electrical Resistivity and Phase Transition. *Phys. Chem. Minerals* **1994**, *21*, 1–5.

15. Miller, E. D.; Nesting, D. C.; Badding, J. V. Quenchable Transparent Phase of Carbon. *Chem. Mater.* **1997**, *9*, 18–22.

16. Yagi, T.; Utsumi, W.; Yamakata, M.-A.; Kikegawa, T.; Shimomura, O. High Pressure In-situ X-ray Diffraction Study of the Phase Transformation from Graphite to Hexagonal Diamond at Room Temperature. *Phys. Rev. B* **1992**, *46*, 6031–6039.

17. Goncharov, A. F. Graphite at High Pressures: Amorphization at 44 GPa. *High Press. Res.* **1992**, *8*, 607–616.

18. Bundy, F. P.; Bassett, W. A.; Weathers, M. S.; Hemley, R. J.; Mao, H.-K.; Goncharov, A. F. The Pressure-temperature Phase and Transformation Diagram for Carbon; Updated Through 1994. *Carbon* **1996**, *34*, 141–153.

19. Jayraman, A. Diamond Anvil Cell and High-pressure Physical Investigations. *Rev. Mod. Phys.* **1983**, ***55***, 65–108.

20. Zha, C. S.; Mao, H. K.; Hemley, R. J. Elasticity of MgO and a Primary Pressure Scale to 55 GPa. *Proc. Nat. Acad. Sci.* **2000**, *97*, 13494–13499.

21. (a) Brown, A.R.G.; Watt, W. *Industrial Carbon and Graphite* (Society of Chemical Industry, London, 1958), p. 86. (b) Brown, A.R.G.; Clark, D.; Estabrook, J. Some Interesting Properties of Pyrolytic Carbon. *J. Less Common Metals* **1959**, *1*, 94–100. (c) Guentert, O.J. X-ray Study of Pyrolytic Graphites. *J. Chem. Phys.* **1962**, *37*, 884–891.

22. Birch, F. Finite Strain Isotherm and Velocities for Single-crystal and Polycrystalline NaCl at High Pressures and 300 °K. *J. Geophys. Res.* **1978**, *83*, 1257–1268.

23. Selvi, E.; Ma, Y.; Askoy, R.; Ertas, A.; White, A. High Pressure X-ray Diffraction Study of Tungsten Disulfide. *J. Phys. Chem. Solids* **2006**, *67*, 2183–2186.

24. Askoy, R.; Ma, Y.; Selvi, E.; Chyu, M. C.; Ertas, A.; White, A. X-ray Diffraction Study of Molybdenum Disulfide to 38.8 GPa. *J. Phys. Chem. Solids* **2006**, *67*, 1914–1917.

25. Hope, K. M.; Vohra, Y. K.; LeBihan, T. Analysis of Anisotropic Compression of Uranium Under High Pressures: a Computational and Experimental Overview. *High Pressure Research* **2005**, *25*, 235–42.

26. Reich, S.; Thomsen, C. Raman Spectroscopy of Graphite. *Phil. Trans. R. Soc. Lond. A* **2004**, *362*, 2271–2288.

27. Ferrari, A. Raman Spectroscopy of Graphene and Graphite: Disorder, Electron-phonon Coupling, Doping and Nonadiabatic Effects. *Solid State Communications* **2007**, *143*, 47–57.

28. Castiglioni, C.; Negri, F.; Rigolio, M.; Zerbi, G. Raman Activation in Disordered Graphites of the A1' Symmetry Forbidden k ≠0 Phone: The Origin of the D Line. *J. Chem. Phys.* **2001**, *115*, 3769–3779.

29. Castiglioni, C.; Tommasini, M.; Zerbi, G. Raman Spectroscopy of Polyconjugated Molecules and Materials: Confinement Effect in One and Two Dimensions. *Philos. Trans. R. Soc. Lond. Ser. A* **2004**, *362*, 2425–2459.

30. Ferrari, A. C.; Robertson, J. Interpretation of Raman Spectra of Disordered and Amorphous Carbon, *Phys. Rev. B* **2000**, *61*, 14095–14107.

31. Tunistra, F.; Koening, J. L. Raman Spectrum of Graphite. *J. Chem. Phys.* **1970**, *53*, 1126–1131.

32. Ghosh, D.; Subhash, F.; Lee, C. H.; Yap, Y. K. Strain-induced Formation of Carbon and Boron Clusters in Boron Carbide Under Dynamic Indentation. *Appl. Phys. Lett.* **2007**, *91*, 061910-1–061910-3.

No. of Copies	Organization
1 ELEC	ADMNSTR DEFNS TECHL INFO CTR ATTN DTIC OCP 8725 JOHN J KINGMAN RD STE 0944 FT BELVOIR VA 22060-6218
1 HC	US ARMY RSRCH LAB ATTN RDRL CIM G T LANDFRIED BLDG 4600 ABERDEEN PROVING GROUND MD 21005-5066
3 HCS	US ARMY RSRCH LAB ATTN IMNE ALC HRR MAIL & RECORDS MGMT ATTN RDRL CIM L TECHL LIB ATTN RDRL CIM P TECHL PUB ADELPHI MD 20783-1197
1 ELEC	US ARMY RSRCH LAB ATTN RDRL WML B J CIEZAK-JENKINS BLDG. 390 ABERDEEN PROVING GROUND MD 21005-5069

TOTAL: 6 (2 ELEC, 4 HCS)

INTENTIONALLY LEFT BLANK.